Instituto de Engenharia de Sistemas e Computadores de Coimbra

Institute of Systems Engineering and Computers

INESC - Coimbra

Cidália C. Fonte, Joaquim Patriarca, José-Paulo Almeida,
Alberto Cardoso, Jacinto Estima, Daniel Silvestre

**Quality assessment of positioning and
orientation data collected by mobile devices**

No. 1   2022

Instituto de Engenharia de Sistemas e Computadores de Coimbra

INESC - Coimbra

Rua Sílvio Lima, Polo II da UC, DEEC; 3030-790 Coimbra; Portugal

www.inescc.pt

This page was intentionally left blank

Quality assessment of positioning and orientation data collected by mobile devices

Cidália C. Fonte [1,2], Joaquim Patriarca[2,3], José-Paulo de Almeida[1,2], Alberto Cardoso[3], Jacinto Estima[4,5], Daniel Silvestre[6,7]

[1] University of Coimbra, Department of Mathematics

[2] Institute of Systems Engineering and Computers (INESC Coimbra)

[3] University of Coimbra, Department of Informatics Engineering, Center for Informatics and Systems, University of Coimbra (CISUC)

[4] IADE, Universidade Europeia

[5] Institute of Systems Engineering and Computers: Investigação e Desenvolvimento em Lisboa (INESC-ID)

[6] Institute for Systems and Robotics, Instituto Superior Técnico, University of Lisbon

[7] Department of Electrical and Computer Engineering, School of Science and Technology, NOVA University of Lisbon

Corresponding author: cfonte@mat.uc.pt

March 2022

Abstract

Mobile devices are increasingly equipped with multiple sensors and computational power to support applications that offer the possibility for citizens to contribute to crowdsourced projects involving the geolocation of individuals or events. However, the quality of the collected data may have impact on the usefulness of the data for specific projects. In this paper, the quality of GNSS-based positioning and compass-based orientation data collected by several mobile devices are assessed and compared. The aim is to determine the impact that the expected errors may have on the data con-tributed by citizens to report wildfires with an app that is under development and identify which approaches are more likely to provide a more reliable geolocation of the observed events. Tests were made with several types of mobile devices regarding the quality of positioning with the embedded GNSS receiver and the compass orientation. Results showed that, even though outliers may occur, errors in geolocation were of several tens of meters and these may vary during the

1

measurements. On the other hand, errors associated with the compass measurements may be of tens of degrees and have a systematic nature, which raises more problems when using these data for the geolocation of critical events, such as wildfires.

1. Introduction

In the advent of smartphones and tablets, the development of mobile applications has made possible inexpensive solutions to various problems. Moreover, fast prototyping of autonomous vehicles controllers and/or algorithms for multi-agent networks of mobile robots can resort to sensor data gathering supported by smartphones. In particular, Global Navigation Satellite System (GNSS) receivers and digital compasses or magnetometers provide the necessary information for sensor fusion for an inertial navigation system to be used in applications such as: navigation [1], georeferencing content [2], robotic formations [3,4], crowdsourced data mobile applications [5], among others. However, the quality of the collected data is a key point for several of these applications.

It is known that the quality of positioning with GNSS receivers is dependent on several aspects, including the type of receivers used (e.g., mono-frequency or double frequency, number of channels, etc.), the number and geometry of the GNSS satellites constellation used to determine the location (assessed with the several aspects of Dilution Of Precision - DOP), the atmospheric effects (mainly the effects of the troposphere and ionosphere) and the effect of the surrounding area (e.g., buildings, trees or water) that may generate signal blocking or reflections and the multipath effect (e.g., [6–8]). The effects of all these factors may range from a few centimetres to hundreds of meters, de-pending on the devices, measurement conditions and location. Single and now also double frequency receivers are available in smartphones, and raw data may be retrieved from the GNSS chipsets in these mobile devices. Therefore, not only code pseudorange but also carrier phase and Doppler GNSS measurements are now accessible, which can be processed in real time or post-processing (e.g., [9–11]).

Several authors investigated the accuracy and precision of positioning with smartphone GNSS receivers. High accuracies and precisions, in some cases comparable to high quality GNSS receivers, have already been reached, even though improvements still need to be done to

decrease the effects of the known error sources. For example, Liu et al. [12] proposed a method based on real-time regional ionospheric model retrieved from dual-frequency GNSS observation data (obtained through CORS – the regional Continuously Operating Reference Stations) to invert the ionospheric model, to correct the GNSS positioning error, and to transmit results to the smartphone so as to achieve re-al-time ionospheric correction. Results showed that the real-time regional ionospheric model can in fact significantly improve positioning accuracy of smartphones, especially in the elevation direction; if compared to Klobuchar model, the improvement effect is more than 34%, and the real-time regional ionospheric model also shortens the convergence time of the elevation direction in 1 min. Uradzinski et al. [13] investigated the positioning accuracy resulting from the carrier phase ambiguity fixing results using the du-al-frequency GNSS receiver available in the Huawai P30 pro smartphone. Commercial post-processing software was used for data processing. The obtained results reached centimetre accuracy. Dabove et al. [10,14] also compared the accuracy and precision of positioning with smartphones and an external GNSS receiver, considering several posi-tioning methods, both in real-time and post-processing. In [10] the authors concluded that with the external GNSS receiver precisions and accuracies of a few centimetres were obtained, while these were worse with the smartphones, reaching a few meters in some cases, due mainly to the measurements noise. Specht et al. [15] analysed the accuracy of the dynamic positioning of six Samsung Galaxy smartphones during vessel manoeu-vring. The telephone positions collected were compared to those of precise GNSS re-ceivers, using corrections from an active geodetic network with an accuracy of 2–3 cm (with p = 0.95). The accuracy statistics for each of the phone models were defined based on approximately 10,000 positions. The study indicates that there are significant differences in the accuracy of positioning as performed by the models in question. Merry and Bet-tinger [16] studied the relative positional accuracy in an urban environment, during two seasons of the year, two times of day, and two perceived WiFi usage periods, using an iPhone 6 device. The average horizontal position error seemed to improve with the time of day (i.e., in the afternoon) and during the leaf-off season. Guo et al. [11] assessed the characteristics of raw multi-GNSS observations from Xiaomi Mi 8 smartphone under static open and dynamic complex environments, not only in terms of Carrier-to-Noise ratio, pseudorange noise, and carrier phase observations, but also the approximate percentage of pseudorange gross errors and carrier phase cycle slips. Given the frequent signal interruptions

and carrier phase cycle slips of raw Xiaomi Mi 8 observations under a complex navigation environment, those authors proposed an improved time-differenced navigation algorithm using raw dual-frequency multi-GNSS measurements from the smartphone. Kinematic experiments were undertaken in both open-sky and GNSS-degraded environments; the proposed time-differenced positioning filter was as-sessed in terms of the positioning accuracy and solution availability. Results in open-sky environment, assisted with L5/E5 observations, showed that the root mean square of the stand-alone horizontal and vertical positioning errors were about 1.22 m and 1.94 m, respectively, with a 97.8% navigation availability; furthermore, in a GNSS-degraded environment, smooth navigation services with accuracies of 1.61 m and 2.16 m in the horizontal and vertical directions were obtained by using multi-GNSS and L5/E5 ob-servations. In addition, [17] showed that for two iPhones 4 and Samsung Galaxy Nexus, the mean location and compass errors are 10 to 30 meters and 10 to 30 degrees, respec-tively. In this paper, we aim to further demonstrate the error characteristics of these inbuilt sensors.

In the realm of robotics, the work of Olivieri de Souza and M. Endler [18] proposed a mobile phone centered control for an autonomous aerial vehicle, where sensor infor-mation was used along with the communication capabilities for the task of coordinating a formation of quadcopters. The study reported in this paper is relevant in the sense that exposes sensors (compass and GNSS receivers) limitations, not only in terrains having large structures, natural bodies of water, where the errors are known to be larger, but also in other regions. Having a characterization of the error statistics and the knowledge of potential solutions to mitigate them is important for other applications, such as those using georeferenced data collected by drones. Regarding the magnetic azimuth measured by an inbuilt digital compass, the measurements may be influenced by external effects and sensor related noise. The former are related to the effect of magnetic fields in the neighbourhood that may influence the measurement, such as the proximity of ferromagnetic materials like cars, metallic con-structions, or electrical currents (e.g, [7,19]). The sensor noise is related to the quality of the sensor itself and the design of the device (i.e., the internal disposition of the hardware). Less studies are available analysing the quality of the orientation data collected with smartphones, both regarding bearing and attitude [20]. However, some studies show that the sensors installed in smartphone devices, which are usually built-in mass production options, may have varying levels of quality, which will influence the accuracy and precision of measurements. Systematic errors may exist in the

measurements and even drift over time (e.g., [21,22]). Odenwald [23] performed an experiment using one device and the measurement of one bearing, and an offset of 3 towards east was obtained. Regarding the measurement of a 90 angle, the author concluded that the relative bearings (angle measurement) was good to about 1 . Other authors such as in [24] have investigated the errors of obtaining the compass reading from GPS signals. It is proposed a method to estimate heading and associated errors and shown how to be minimized. However, to obtain errors of below 1° it is required to have a longer distance between the two antennas receiving the GPS signal, which is not feasible in mobile phones.

One of the natural fields of application for smartphone-based positioning is low-cost mobile mapping systems. As initial studies have shown, smart-devices may be effectively employed in such applications [25,26]. Applications requiring the collective effort of citizens along with researchers can be tackled using crowdsourcing mobile applications to gather data. Many of these projects are available, such as the OpenStreetMap project (https://www.openstreetmap.org/), Wikimapia (http://wikimapia.org/) or Geograph (https://www.geograph.org/) [27,28]. The project FireLoc (https://fireloc.org/), under development, aims at collecting locations of forest fires using crowdsourced data, through the triangulation of contributors' localization and orientation towards the event. GNSS receiver takes care of the localization, whereas orientation can be obtained from the built-in digital compass. However, a major issue is that noise in the measurements can render the sensor fusion algorithm useless if outliers are not accommodated appropriately and the characterization of the error dynamics and probability distributions involved are absent. This paper aims at presenting a comprehensive experimental test using different mobile devices and the respective characterization for FireLoc system. However, the obtained results may also be of use for robotic applications alike.

In this paper, we investigate the variability of the geolocation and bearing errors when measured at the same location with different mobile devices. Two different ex-periments were set up and made at four sites. A statistical analysis of the geolocation and orientation errors was made. Results showed that outliers occurred both in the geolocation and orientation, however different devices showed to have different levels of reliability. The magnitude of the obtained geolocation errors showed to be less problematic than the orientation error when these data are to be used in crowdsourced projects, such as the FireLoc project, where the aim is to geolocate observed

events based on the geolocation of several observers and the bearings measured when facing the event.

The remainder of this paper is organized as follows. The equipment used in the experiments is presented in Section 2, as well as the performed tests. The main results are presented in Section 3, and these are discussed in Section 4. Section 5 concludes with some final remarks and directions of future work.

2. Materials and Methods

In this chapter, we describe the equipment used in this study, as well as the adopted methodology, which involves two experiments ran in four points located at two different areas.

2.1 Equipment

Five different mobile devices were used in the tests performed. Four smartphones with different brands and models and a Tablet. The device's characteristics are listed in Table 1, along with the version of the operating system used.

Table 1. Equipment used in the experiments.

Brand	Model	Version of operating system
Samsung Galaxy A70	SM-A705FN/DS	Android 10
Huawei	VFD 600	Android 6.0.1
Samsung Galaxy Tablet S5e	SM-T725	Android 9
ASUS Zenfone 4 Selfie Pro	ASUS_Z01MD	Android 7.1.1
Nokia 8	TA-1004	Android 9

No particular strategy was considered in the selection of the used devices, as the aim was to assess the variability of the collected data using devices with different characteristics. However, only devices with the Android operating system were used, so that the same compass app could be used in all measurements. The app used was the basic version of the Digital Compass melon soft, made available by Google Commerce Ltd. since 2015. The functions available in this app include [29].

- The display of the True or Magnetic North direction and the angle between the device orientation (heading) relative to either one, which are called, respectively, the true bearing and the magnetic bearing;
- Display of the latitude and longitude of the device location.

An analogue compass was also used to measure the magnetic bearings.

2.2. Experiment description

Two experimental procedures were set up - Experiment 1 and Experiment 2 - to assess: 1) the accuracy of the coordinates obtained in several locations with the GNSS receivers embedded in the mobile devices; 2) the accuracy and precision of the bearings provided by the mobile devices; and 3) how the positioning errors may affect the bearing computation using the coordinates of two or three points aligned along the direction whose bearing is to be computed. Both procedures were tested in several locations using the mobile devices presented in Subsection 2.1. All location measurements consist of the geographical coordinates latitude (φ) and longitude (λ) in the geographical reference system WGS 89 (World Geodetic System 1989), which were then converted to projected coordinates (XP, YP) in the reference system PT-TM06 ETRS89 (EPSG code 3763). The orientation measurements where the true bearings expressed in sexagesimal degrees (°).

2.2.1. Experiment 1

Experiment 1 consisted in placing the mobile device in only one location P each time the experiment was made. The coordinates (XP, YP) of point P were measured 20 times, changing, between each measurement, the heading of the device between orientations O1 and O2, which are perpendicular to each other (see Figure 1).
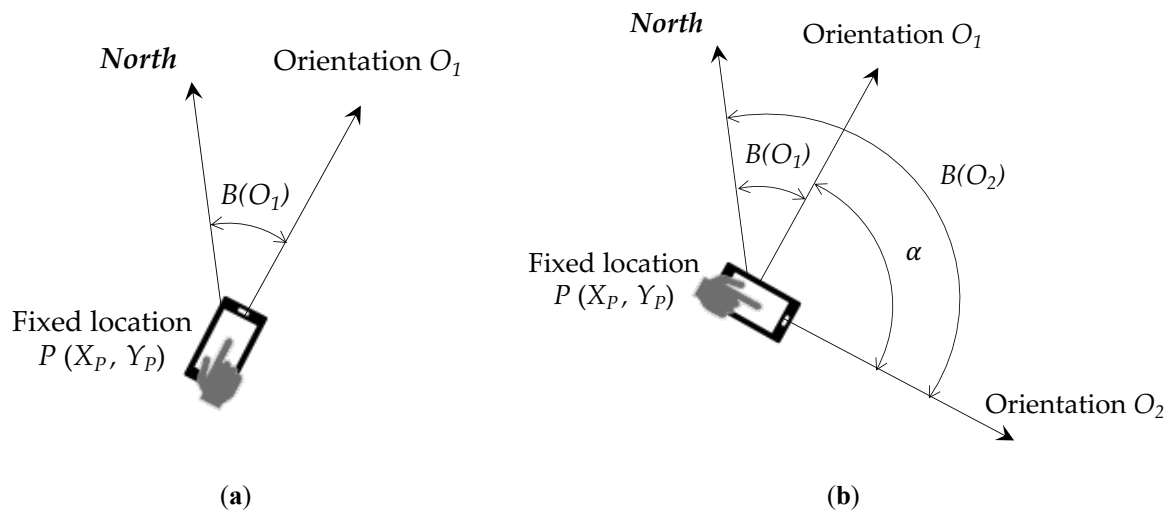
Figure 1. Illustration of Experiment 1: (a) The coordinates of the point P are registered as well as the true bearing of the orientation O1 - B(O1); (b) The coordinates of point P are measured and registered again, as well as the true bearing of the direction O2 - B(O2). Directions O1 and O2 are known to be perpendicular.

The magnetic bearings of these orientation were measured with the mobile devices and the analogue compass. This procedure enabled the computation of angle α with equation (1), where B(O1) and B(O2) were, respectively, the measured bearing of the orientation O1 and O2. As orientations O1 and O2 are perpendicular, angle α should be approximately 90°.

$$\alpha = B(O_2) - B(O_1). \tag{1}$$

If no measurement errors existed, all 20 measurements of (X_P, Y_P) should be equal, as well as the bearings corresponding to the orientations O_1 and O_2 (10 measurements of each bearing). The angle α computed using the bearings measured with the analogue and the digital compasses should also be equal.

2.2.2. Experiment 2

Experiment 2 consisted of sequences of four measurements in three aligned locations $P_{Central}$, $P_{Forward}$ and $P_{Backward}$, which were repeated 5 times, generating the measurements of the location (X_i, Y_i) of points P_i, where $i=1,...,20$ (see Figure 2).
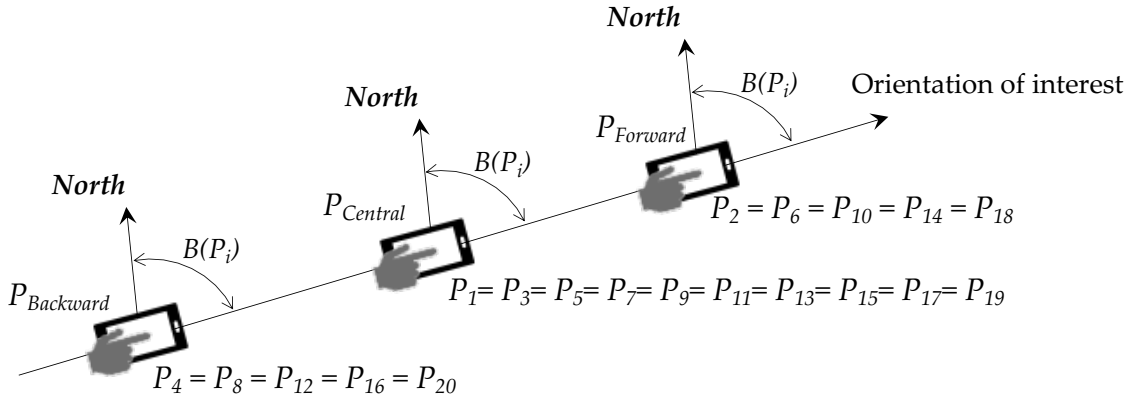
Figure 2. Illustration of Experiment 2.

The orientation of the device was maintained in all measurements, and the bearing $B(P_i)$ (with $i=1,...,20$) registered. In this procedure, the coordinates (X_i, Y_i) and orientation at $P_{Central}$ were measured 10 times (points P_i, with odd values of i), while the coordinates and bearing at the extreme points, $P_{Forward}$ and $P_{Backward}$, were measured 5 times each.

If no measurement errors existed, all bearing measurements within this experiment for each set of points $P_{Central}$, $P_{Forward}$ and $P_{Backward}$ should be equal, as the orientation was kept unchanged, and

the coordinates obtained for each of the points $P_{Central}$, $P_{Forward}$ and $P_{Backward}$ should also be the same.

2.3. Observation sites

The tests made with Experiments 1 and 2 were repeated in several locations with several mobile devices. In some cases, the devices were in flight mode, to determine if the on/off state of the communication equipment could have some influence over the obtained results. The chosen points were located in two different areas described in subsubsections 2.3.1 and 2.3.2. As one of the aims of this study is to assess the variability of the measurements made by citizens when contributing with data to projects relying on their contributions, the selected locations do not have particularly good or bad environmental conditions for these types of observations. However, no points were selected close to water bodies, between buildings or trees, as it is known that these may have large influences over the quality of positioning due to either multipath or signal blocking [9,23,25].

2.3.1. Study Area A

Study area A is located in Pole II of the University of Coimbra (UC), close to the Department of Civil Engineering. Figure 3 shows the area and its surrounds, as well as the location of the selected points $UC_{Central}$, $UC_{Forward}$ and $UC_{Backward}$.

Figure 3. Study area A and points $UC_{Central}$, $UC_{Forward}$ and $UC_{Backward}$.

The reference coordinates of these points were extracted from an orthophoto with a spatial resolution of 25 cm, made available by the Portuguese national mapping agency "Direção Geral do Território" (DGT) through a Web Feature Service (WFS) [30]. Table 2 shows these coordinates, in the reference system PT-TM06 ETRS 89 (EPSG code 3763).

2.3.2. Study Area B

Study area B is located near the Aerodrome (A) of Cernache. Figure 4 shows the area and its surrounds, as well as the location of the three sets of points $Ai_{Central}$, $Ai_{Forward}$ and $Ai_{Backward}$ ($i = 1,2,3$) used in this analysis. The reference coordinates of these points (shown in Table 2) were also extracted from the orthophotos with a spatial resolution of 25 cm made available by DGT. All the measurements made at points $A2_{Central}$, $A2_{Forward}$ and $A2_{Backward}$ were made with the mobile devices in flight mode, to assess if that might have any influence over the obtained results.
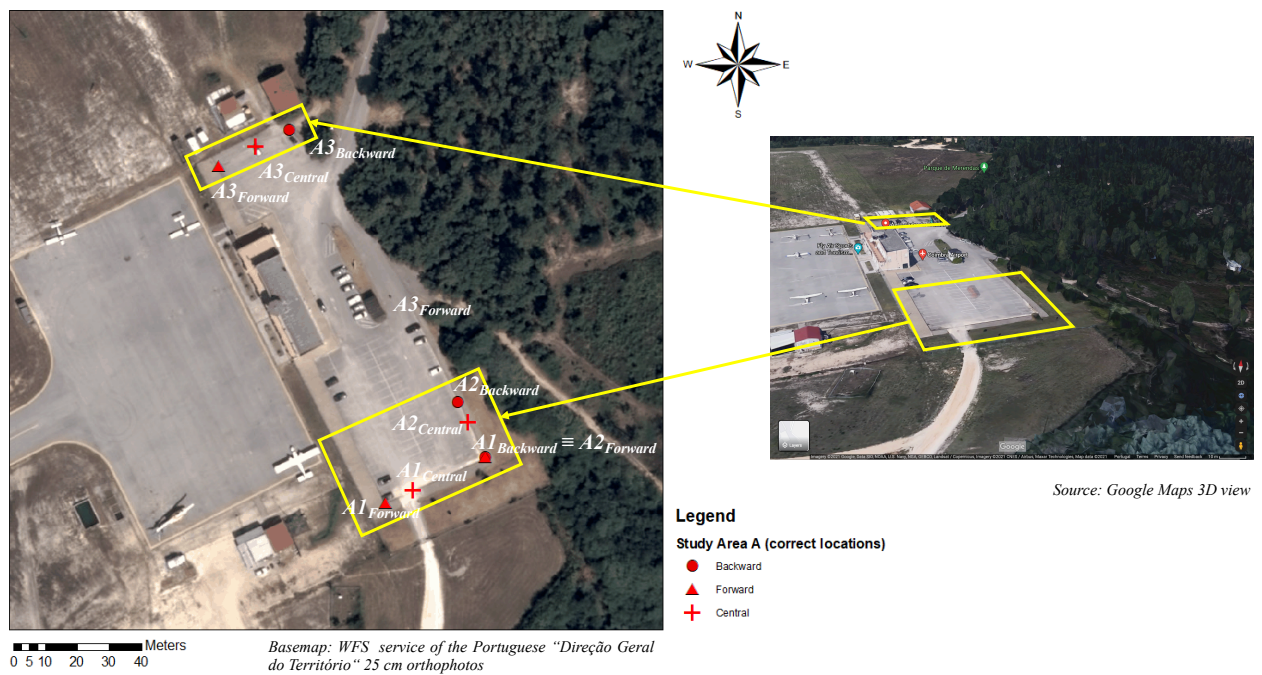
Figure 4. Study area B and points $Ai_{Central}$, $Ai_{Forward}$ and $Ai_{Backward}$ ($i = 1,2,3$).

Table 2. Reference coordinates of the points used in the experiments (reference system: EPSG code 3763).

Study area	Point	X (m)	Y (m)
Study area A	$UC_{Central}$	-24000.78	57443.88
	$UC_{Forward}$	-24022.15	57443.86
	$UC_{Backward}$	-23981.50	57443.88
Study area B	$A1_{Central}$	-28447.35	54250.04
	$A1_{Forward}$	-28452.56	54247.84
	$A1_{Backward}$	-28425.33	54260.06
	$A2_{Central}$	-28430.83	54271.08
	$A2_{Forward}$	-28425.33	54260.06
	$A2_{Backward}$	-28433.84	54277.41
	$A3_{Central}$	-28499.61	54355.73
	$A3_{Forward}$	-28509.59	54350.99
	$A3_{Backward}$	-28491.16	54360.03

2.4. Assessment of the geolocation accuracy and precision

To assess the accuracy and precision of the geolocation measured n times with the mobile devices in Experiments 1 and 2 at each point P, the distance $D(P, P_j)$ between the coordinates obtained at measurement j (X_{Pj}, Y_{Pj}) (for $j = 1,...,n$) and the reference coordinates (X_P, Y_P) (listed in Table 2) where computed using equation (2).

$$D(P, P_j) = \sqrt{\left(X_{Pj} - X_P\right)^2 + \left(Y_{Pj} - Y_P\right)^2}. \tag{2}$$

Then, for the n repeated measurements of the location of point P, the mean $\overline{D(P, n)}$ of the obtained distances $D(P, P_j)$ was computed with equation (3), which provides information about the measurement's accuracy.

$$\overline{D(P, n)} = \sum_{j=1}^{n} \frac{D(P, P_j)}{n}. \tag{3}$$

The minimum, the maximum and the standard deviation $SD[D(P, n)]$, computed using equation (4), provide information about the precision of the measurements.

$$SD[D(P, n)] = \sqrt{\frac{\sum_{j=1}^{n}\left(D(P, P_j) - \overline{D(P, n)}\right)^2}{n - 1}}. \tag{4}$$

11

The analysis of the results was made by mobile device, number of repeated measurements *n* and observed points of study areas A and B.

2.5. Assessment of orientation accuracy and precision

This analysis was made with two approaches, the first aimed to assess the accuracy and precision of the bearings measured with the digital compasses when compared with the values obtained with an analogue compass. The second aimed to assess if, even though systematic errors may exist in the bearings measured with the digital compass, these were kept relatively stable, so that the difference between two measured bearings is similar to the real angle a computed with equation (1) in Experiment 1 when measured with the analogue compass (α_{Analog}).

2.5.1. Orientation variability

For Experiment 1 described in section 2.2.1, for each considered point and equipment, the means ($\overline{B(O_1)}$ and $\overline{B(O_2)}$) and the standard deviations ($STD[B(O_1)]$ and $STD[B(O_2)]$) of the measured bearings for orientations O_1 and O_2 were computed. Then, the difference (B_{Diff}) between the bearings measured with the analogue compass ($B_{Analog}(O_1)$ and $B_{Analog}(O_2)$), and the mean value obtained for each orientation was computed (see equation (5), where *m* is equal to 1 or 2). This enabled the assessment of the accuracy of the bearings measured with the digital compasses.

$$B_{Diff}(O_m) = B_{Analog}(O_m) - \overline{B(O_m)}. \tag{5}$$

To assess the magnitude and variability of B_{Diff} by mobile device, the mean ($\overline{B_{Diff}(O_m)}$), and standard deviation ($SD(B_{Diff}(O_m))$) of the values obtained with the measurements made in all considered points and with all devices was also computed, as well as the minimum and maximum of their absolute values.

For Experiment 2, the variability and accuracy of the bearing measured with each mobile device at each location was assessed by computing the mean ($\bar{B}$) and the standard deviation ($SD(B)$) of the bearings B measured with the mobile devices and the difference B_{Diff} computed with equation (6), where B_{Analog} is the bearing measured with the analogue compass.

$$|B_{Diff}| = |B_{Analog} - \bar{B}|. \tag{6}$$

2.5.2. Variability of the difference of bearings

To analyse the accuracy and precision of angle a measured with the digital compasses, a was computed for each location considered in Experiment 1, with each mobile device, with the successive measured bearings $B(O_1)$ and $B(O_2)$. When the process was repeated n times, n values a_i ($i=1,...,n$) were obtained. Then, the mean ($\bar{\alpha}$) and the standard deviation ($SD(\alpha)$) were computed. The difference between the mean value $\bar{\alpha}$ and the magnetic bearing measured with the analogue compass (α_{Analog}) were computed for all points and all mobile devices using equation (7).

$$\alpha_{Diff} = \alpha_{Analog} - \bar{\alpha}. \tag{7}$$

As made for the bearing, to assess the magnitude and variability of α_{Diff}, the minimum, maximum, mean ($\overline{\alpha_{Diff}}$) and standard deviation ($SD(\alpha_{Diff})$) of the values obtained with the measurements made in all considered points and with all devices was computed.

3. Results

The results obtained with the measurements made within the two experiences described in the previous section are presented separately for the geolocation and orientation. As the aim of this paper is not to compare the performance of each mobile device in particular, but how the results may change with different devices, the brands and models are ignored and the devices represented simply as MD_k, with $k = 1,...,5$.

3.1. Geolocation

Figure 5 shows the measured geolocation of all points $UC_{Central}$, $UC_{Forward}$ and $UC_{Backward}$ with Experiments 1 and 2. A total of 150 measurements were made at point $UC_{Central}$ considering all mobile devices and Experiments 1 (100) and 2 (50). The geolocation of points $UC_{Forward}$ and $UC_{Backward}$ was only measured with Experiment 2, and each point was measured a total of 25 times when considering all mobile devices used.
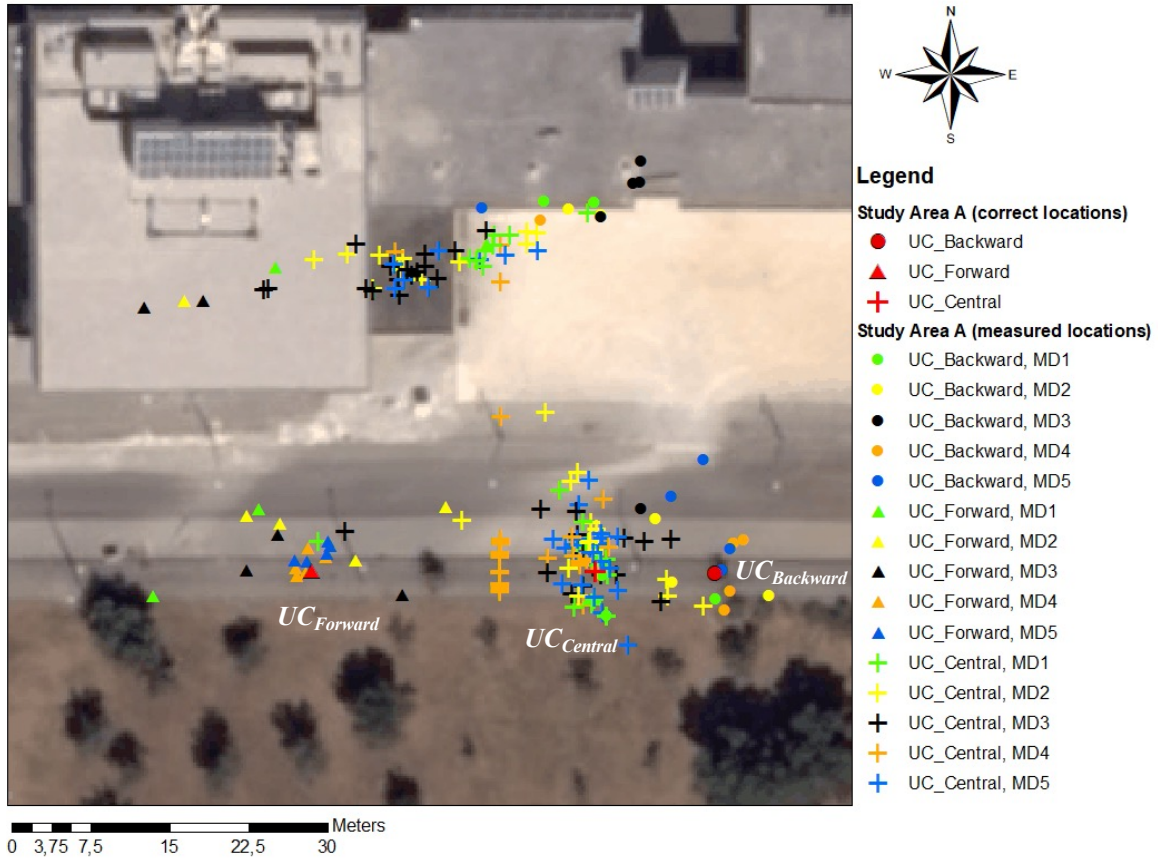
Figure 5. Geolocation of the real and measured points of study area A: $UC_{Central}$ obtained with Experiment 1 and Experiment 2, as well as $UC_{Forward}$ and $UC_{Backward}$ obtained with Experiment 2. The different colours represent the mobile devices MD_k ($k = 1,...,5$) used to collect the data.

The same measurements were repeated for location A_1, A_2 and A_3 at study area B, and the geolocation of the obtained coordinates are shown in, respectively, Figures 6 to 8.

From the analysis of Figures 5 to 8 stands out that sometimes a systematic deviation of the geolocation in the direction of the nearby buildings (even when the buildings are small, as in Study Area B) was observed. This occurred with all mobile devices and almost all points. The likely explanation for this effect is the multipath effect that may occur due to the reflection of the GNSS signal emitted by the satellites in the nearby buildings. Some outliers can also be observed, especially for Study area B (Figure 6(a), Figure 7(a) and Figure 8(a)).
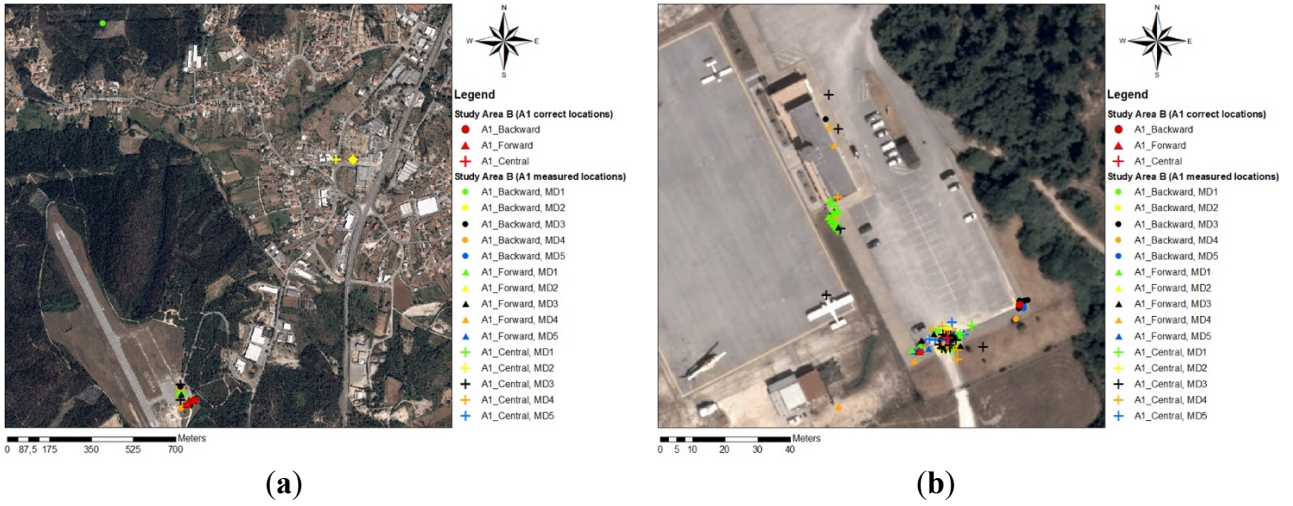
Figure 6. Geolocation of the real and measured points of study area B: $A1_{Central}$ obtained with Experiment 1 and Experiment 2, as well as $A1_{Forward}$ and $A1_{Backward}$ obtained with Experiment 2. The different colours represent the mobile devices MD_k ($k = 1,...,5$) used to collect the data.
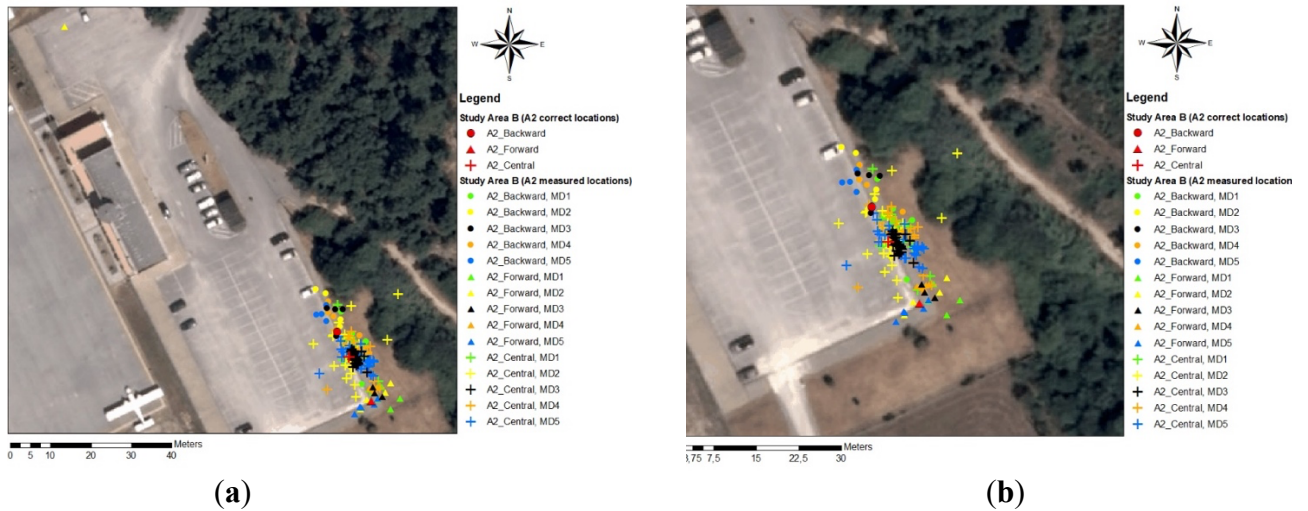
Figure 7. Geolocation of the real and measured points of study area B: $A2_{Central}$ obtained with Experiment 1 and Experiment 2, as well as $A2_{Forward}$ and $A2_{Backward}$ obtained with Experiment 1. The different colours represent the mobile devices MD_k ($k = 1,...,5$) used to collect the data.
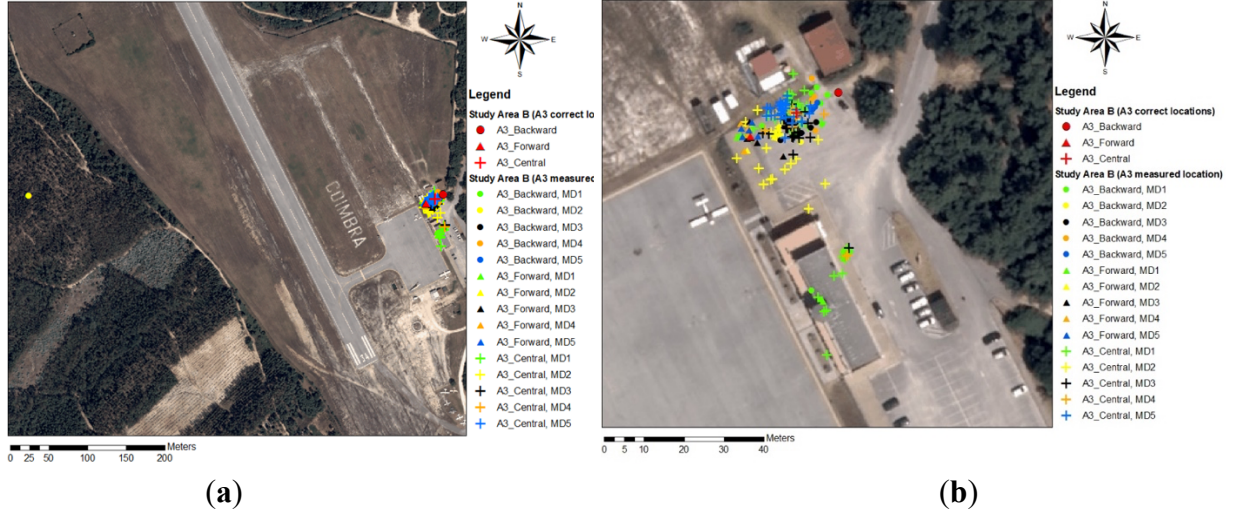
Figure 8. Geolocation of the real and measured points of study area B: $A3_{Central}$ obtained with Experiment 1 and Experiment 2, as well as $A3_{Forward}$ and $A3_{Backward}$ obtained with Experiment 1. The different colours represent the mobile devices MD_k ($k = 1,...,5$) used to collect the data.

Tables 3 to 5 show, per mobile device and point, the mean $(\overline{D(P,n)})$, the standard deviations $(STD[D(P,n)])$ and the minimum and maximum distances $D(P,P_j)$ between the measured (P_j for $j = 1,...,n$) and the known (P) geolocation of the points, computed with equation (2), for $n=20$ (Table 3), $n=10$ (Table 4) and $n=5$ (Table 5), where n is the number of repeated measurements per point.

The analysis of Tables 3 to 5 show clearly the outliers. In Tables 3 and 4 the measurements made at point $A1_{Central}$ with the device M_2 have much larger errors than all other measurements (see also Figure 6(a) – yellow points). A similar behaviour is observed in Table 5 for points $A1_{Backward}$ and $A1_{Forward}$ for MD_2 (Figure 6(a)), but also at $A1_{Backward}$ for MD_1 with an even larger maximum distance to the correct location (Figure 6(a) – green point away from the true location), and with a smaller deviation for $A3_{Backward}$ with MD_2 (Figure 8(a)). This shows that the geolocation with smartphones, in some cases, may have errors that may reach more than 1km (the maximum observed distance was 1.616 km). This was observed with two MD, only one time with MD_1, but several times with MD_2.

Table 6 shows the mean distance to the reference location $\overline{D(P,n)}$ and the standard deviation $SD[D(P,n)]$ by mobile device and points measured with $n = \{20,10,5\}$. The results show that, in general, the more repeated measurements are made the lower is the mean distance to the

reference and the standard deviation of the measurements. However, a few exceptions are observed, where the differences between the obtained values are very small, and when outliers are present.

The obtained results show that in most cases the mean distance to the reference location is up to 20 or 30 meters. However, for some mobile devices these values are smaller than 10m. This is also observed for the measurements made at location A_2, where the measurements were made with the mobile devices in flight mode.

Table 3. Statistical analysis by mobile device MD_k ($k = 1,...,5$) of the distance $D(P, P_j)$ (in meters) between the measured coordinates P_j (with $j = 1,...,n$) and the reference coordinates of P when performing n measurements, with $n = 20$, where $\overline{D(P,n)}$ is the mean distance, $SD[D(P,n)]$ is the standard deviation, and $min(D(P,P_j))$, and $max(D(P,P_j))$ are, respectively, the minimum and maximum distances obtained. P corresponds to points $UC_{Central}$ and points $Ai_{Central}$ ($i = 1,2,3$).

Point	Mobile device	$\overline{D(P,20)}$	$SD[D(P,20)]$	$min(D(P,P_j))$	$max(D(P,P_j))$
$UC_{Central}$	MD_1	12	10	6.2	35
	MD_2	19	12	4.8	33
	MD_3	21	12	2.8	36
	MD_4	6	9	1.7	31
	MD_5	13	10	4.2	31
$A1_{Central}$	MD_1	27	24	0.4	54
	MD_2	854	571	2.2	1221
	MD_3	11	21	0.8	73
	MD_4	5	12	0.7	55
	MD_5	2	2	0.4	7
$A2_{Central}$	MD_1	3	3	0.5	13
	MD_2	5	4	0.7	12
	MD_3	2	1	0.8	3
	MD_4	4	2	1.5	8
	MD_5	4	1	1.8	7
$A3_{Central}$	MD_1	30	15	0.1	46
	MD_2	9	6	1.9	24
	MD_3	3	2	1.0	6

Table 4. Statistical analysis by mobile device MD_k ($k = 1,...,5$) of the distance $D(P, P_j)$ (in meters) between the measured coordinates P_j (with $j = 1,...,n$) and the reference coordinates of P when performing n measurements, with $n = 10$, where $\overline{D(P, n)}$ is the mean distance, $SD[D(P, n)]$ is the standard deviation, and $min(D(P, P_j))$, and $max(D(P, P_j))$ are, respectively, the minimum and maximum distances obtained. P corresponds to points $UC_{Central}$ and points $Ai_{Central}$ ($i = 1,2,3$).

Point	Mobile device	$\overline{D(P, 10)}$	$SD[D(P, 10)]$	$min(D(P, P_j))$	$max(D(P, P_j))$
$UC_{Central}$	MD_1	18	11	2.5	39
	MD_2	18	12	4.7	38
	MD_3	21	11	4.1	40
	MD_4	10	8	0.3	38
	MD_5	15	11	0.4	42
$A1_{Central}$	MD_1	33	25	1.4	56
	MD_2	1221	0	1200	1221
	MD_3	14	27	0.5	84
	MD_4	9	23	0.2	75
	MD_5	1	1	0.3	5
$A2_{Central}$	MD_1	4	3	1.5	10
	MD_2	4	6	0.3	19
	MD_3	2	2	0.6	6
	MD_4	4	4	0.7	11
	MD_5	4	2	1.6	9
$A3_{Central}$	MD_1	33	22	0.2	61
	MD_2	8	7	0.8	19
	MD_3	9	10	0.9	36
	MD_4	11	15	0.2	38

Table 5. Statistical analysis by mobile device MD_k ($k = 1,...,5$) of the distance $D(P, P_j)$ (in meters) between the measured coordinates P_j (with $j = 1,...,n$) and the reference coordinates of P when performing n measurements, with $n = 5$, where $\overline{D(P, n)}$ is the mean distance, $SD[D(P, n)]$ is the standard deviation, and $min(D(P, P_j))$, and $max(D(P, P_j))$ are, respectively, the minimum and maximum distances obtained. P corresponds to points $UC_{Forward}$ or $UC_{Backward}$ and points $Ai_{Forward}$ and $Ai_{Backward}$ ($i = 1,2,3$).

Mobile device	Point	$\overline{D(P, 5)}$	$SD[D(P, 5)]$	$min(D(P, P_j))$	$max(D(P, P_j))$
MD_1	$UC_{Backward}$	20	17	2.5	39
	$UC_{Forward}$	23	12	7.1	36
MD_2	$UC_{Backward}$	18	17	4.7	38
	$UC_{Forward}$	12	10	5.0	28
MD_3	$UC_{Backward}$	32	13	9.8	40
	$UC_{Forward}$	15	12	4.1	29
MD_4	$UC_{Backward}$	10	16	1.9	38
	$UC_{Forward}$	2	1	0.3	3
MD_5	$UC_{Backward}$	13	17	0.4	42
	$UC_{Forward}$	3	1	1.3	4
MD_1	$A1_{Backward}$	348	709	1.4	1616
	$A1_{Forward}$	33	25	4.1	51
MD_2	$A1_{Backward}$	1201	0	1200	1201
	$A1_{Forward}$	1226	0	1226	1226
MD_3	$A1_{Backward}$	18	36	1.3	83
	$A1_{Forward}$	13	19	3.2	46
MD_4	$A1_{Backward}$	27	34	0.2	65
	$A1_{Forward}$	18	28	3.3	69
MD_5	$A1_{Backward}$	1	0	0.3	1
	$A1_{Forward}$	5	2	2.0	7
MD_1	$A2_{Backward}$	6	5	2.4	14
	$A2_{Forward}$	6	4	0.9	13
MD_2	$A2_{Backward}$	7	5	1.0	12
	$A2_{Forward}$	27	52	1.7	120
MD_3	$A2_{Backward}$	5	2	1.5	7
	$A2_{Forward}$	6	5	2.0	12
MD_4	$A2_{Backward}$	5	2	3.8	8
	$A2_{Forward}$	3	0	2.5	3
MD_5	$A2_{Backward}$	6	1	3.9	7
	$A2_{Forward}$	3	2	0.9	6
MD_1	$A3_{Backward}$	23	24	1.8	50
	$A3_{Forward}$	19	22	0.2	46
MD_2	$A3_{Backward}$	115	233	7.9	533
	$A3_{Forward}$	6	4	0.8	10
MD_3	$A3_{Backward}$	9	3	5.9	15
	$A3_{Forward}$	4	4	0.9	10
MD_4	$A3_{Backward}$	4	3	1.8	8
	$A3_{Forward}$	2	2	0.2	4

Table 6. Statistical analysis by mobile device MD_k ($k = 1,...,5$) of the distance $D(P, P_j)$ between the measured coordinates P_j (with $j = 1,...,n$) and the reference coordinates of P when performing n measurements, with $n = \{20,10,5\}$, where $\overline{D(P, n)}$ is the mean distance, $SD[D(P, n)]$ is the standard deviation, and $min(D(P, P_j))$, and $max(D(P, P_j))$ are, respectively, the minimum and maximum distances obtained. P corresponds to points $UC_{Central}$, $UC_{Forward}$ or $UC_{Backward}$ and points $Ai_{Central}$, $Ai_{Forward}$ and $Ai_{Backward}$ ($i = 1,2,3$). At each cell of the table the values on the left are computed with all observations and the values on the right are computed excluding the outliers identified above.

Mobile Device	$\overline{D(P,20)}$	$\overline{D(P,10)}$	$\overline{D(P,5)}$	$SD[D(P,20)]$	$SD[D(P,10)]$	$SD[D(P,5)]$	$min(D(P,P_j))$	$max(D(P,P_j))$
MD_1	18 / 18	22 /22	60 /19	13 /13	15 /15	102 /16	0.1	1616 /61
MD_2	222 /11	313 /10	327 /11	148 /7	6 /8	40 /9	0.3	1226 /46
MD_3	9 /9	11 /11	13 /13	9 /9	13 /13	12 /12	0.5	84 /84
MD_4	4 /4	8 /8	9 /9	6 /6	12 /12	11 /11	0.2	75 /75
MD_5	5 /5	5 /5	4 /4	3 /3	4 /4	3 /3	0.3	42 /42

3.2. Orientation

Table 7 shows the variability of the bearing measured with the mobile devices' compass, expressed by the mean and the standard deviation computed with the 10 measurements in each direction O_1 and O_2. The difference B_{Diff} between the mean bearings and the bearings measured with the analogue compass were computed using equation (5). The results are grouped by mobile device, orientation O_1 and O_2 and observation point.

The results in Table 7 show that the standard deviation obtained for each orientation, at each location by all the devices is relatively small. The largest value is 8.1°, but for 27 out of the 36 obtained values, it is equal or smaller than 1°. This shows that the repeated measurements in most cases did not change much. However, the difference between the mean value and the analogue measurement of the bearing in some cases reaches more than 20° (twice with MD_2 and one time with MD_1), achieving a maximum of 27° at $A2_{Central}$ with MD_2.

Table 8 shows the mean $(\overline{B_{Diff}(O_m)})$, standard deviation $(SD(B_{Diff}(O_m)))$, minimum and maximum of the absolute values of $B_{Diff}(O_m)$, respectively $min(|B_{Diff}(O_m)|)$ and $max(|B_{Diff}(O_m)|)$, grouped by mobile device. These results show that mobile devices MD_4 and MD_5 gave better results regarding all statistics. However, both the minimum and maximum differences were obtained for mobile device MD_2, which shows a large variability, and had already given low reliability in the results obtained for the geolocation.

Table 9 shows the variability of the orientation measured with each mobile device at each location in Experiment 2, expressed by the mean of the measured bearing B, the standard deviation and the between the analogue bearing and the mean of the measured values, computed with equation (6). The results also confirm that small values of the standard deviation were obtained, which means that the measurements were precise, but the accuracy of the measurements is much smaller. The 19 results obtained for $|B_{Diff}|$ varied between a minimum of 1° up to a maximum of 20.6°. The value corresponding to the first quartile is 2.2°, the second quartile 5.4° and the third quartile 9.7°. Therefore, in one quarter of the cases the error was larger than almost 9.7° and the larger deviations were obtained with different mobile devices at different locations, but the mobile device showing better results was MD_4.

Given the variability of geolocations obtained in both experiments between repeated measurements at the same points (see Figures 5 to 8), the computation of the bearing with successive points $P_{Central}$, $P_{Forward}$ and $P_{Central}$, $P_{Backward}$ of Experiment 2 may result in errors so large (achieving in some cases more than 40°) that they were considered to be useless for the purpose of obtaining the bearing defined by the obtained locations. Therefore, the detailed analysis of their variability is not presented here in detail.

Table 7. $B_{Analog}(O_m)$, with $m = 1,2$, is the bearing measured with the analogue compass. The obtained values are shown by locations $UC_{Central}$ and points $Ai_{Central}$ $(i = 1,2,3)$ considered at Experiment 1, for orientations O_1 and O_2. $\overline{B(O_m)}$ is the mean value and $STD[B(O_m)]$ the standard deviation of the bearings measured with the mobile devices MD_k $(k = 1,...,5)$ digital compasses', computed with the 10 measurements made at each location for each orientation. $B_{Diff}(O_m)$ is the difference between the analogue bearing and the mean bearing obtained for each orientation (see equation (5)). All values are expressed in degrees.

Point	Orientation	$B_{Analog}(O_m)$	Mobile device	$\overline{B(O_m)}$	$STD[B(O_m)]$	$B_{Diff}(O_m)$
$UC_{Central}$	O_1	275	MD_1	296.8	0.8	-21.8
			MD_2	272.7	2.1	2.3
			MD_3	281.0	1.2	-6.0
			MD_4	273.1	0.6	1.9
			MD_5	272.2	0.6	2.8
	O_2	5	MD_1	357.2	0.8	7.8
			MD_2	4.9	1.9	0.1
			MD_3	352.7	1.2	12.3

			MD_4	5.4	0.8	-0.4
			MD_5	4.4	0.7	0.6
$A1_{Central}$	O_1	250	MD_1	241.0	0.0	9.0
			MD_2	259.7	8.1	-9.7
			MD_3	252.9	0.3	-2.9
			MD_4	255.4	1.0	-5.4
			MD_5	240.7	0.7	9.3
	O_2	340	MD_1	336.1	0.7	3.9
			MD_2	344.0	2.8	-4.0
			MD_3	335.1	0.3	4.9
			MD_4	335.2	1.6	4.8
			MD_5	336.0	0.8	4.0
$A2_{Central}$	O_1	250	MD_1	246.4	0.7	3.6
			MD_2	222.7	0.5	27.3
			MD_3	248.1	0.7	1.9
			MD_4	249.4	0.8	0.6
			MD_5	249.2	0.6	0.8
	O_2	340	MD_1	332.4	0.7	7.6
			MD_2	333.4	1.1	6.6
			MD_3	325.8	0.8	14.2
			MD_4	332.9	0.6	7.1
			MD_5	333.0	0.7	7.0
$A3_{Central}$	O_1	250	MD_1	253.0	0.9	-3.0
			MD_2	229.2	0.4	20.8
			MD_3	239.5	1.0	10.5
	O_2	340	MD_1	335.5	0.5	4.5
			MD_2	336.5	2.3	3.5
			MD_3	326.6	0.7	13.4

Table 8. $\overline{B_{Diff}(O_m)}$ is the mean of $B_{Diff}(O_m)$, computed for all location by mobile device MD_k ($k = 1,...,5$), $SD(B_{Diff}(O_m)$ is the standard deviation of the same values, and $min(|B_{Diff}(O_m)|)$ and $max(|B_{Diff}(O_m)|)$ are, respectively, the minimum and the maximum of the absolute values of $B_{Diff}(O_m)$.

Mobile device	$\overline{B_{Diff}(O_m)}$	$SD(B_{Diff}(O_m))$	$min(|B_{Diff}(O_m)|)$	$max(|B_{Diff}(O_m)|)$
MD_1	7.7	4.9	3.0	21.8
MD_2	9.3	6.8	0.1	27.3
MD_3	8.3	3.3	1.9	14.2
MD_4	3.4	2.0	0.4	7.1
MD_5	4.1	2.5	0.6	9.3

Table 9. B_{Analog} is the bearing measured with the analogue compass. The obtained values are shown by locations UC and points Ai ($i = 1,2,3$) considered at Experiment 2. $\bar{B}$ is the mean

value and $STD(B)$ the standard deviation of the bearings measured with the mobile devices MD_k ($k = 1,...,5$) digital compasses', computed with the 20 measurements made at points *Central*, *Forward* and *Backward* at each location. B_{Diff} is the difference between the analogue bearing and the mean bearing obtained at each location (see equation (6)). All values are expressed in degrees.

Point	Mobile device	B_{Analog}	$\overline{B}$	$SD(B)$	$\lvert B_{Diff} \rvert$
UC	MD_1	275	294.2	0.8	19.2
	MD_2		269.6	1.4	5.4
	MD_3		278.0	0.6	3
	MD_4		272.4	0.5	2.6
	MD_5		270.8	0.6	4.2
A1	MD_1	250	240.6	1.1	9.4
	MD_2		248.4	4.1	1.6
	MD_3		249.0	0.3	1
	MD_4		249.0	0.4	1
	MD_5		240.4	1.5	9.6
A2	MD_1	160	152.0	1.5	8
	MD_2		168.2	1.1	8.2
	MD_3		149.4	1.0	10.6
	MD_4		161.8	0.7	1.8
	MD_5		150.0	1.3	10
A3	MD_1	250	253.4	1.5	3.4
	MD_2		229.4	1.5	20.6
	MD_3		240.2	1.4	9.8
	MD_4		248.4	1.3	1.6

The results regarding the measurement of angle a_i ($i=1,...,n$), in Experiment 1, are shown in Table 10. The difference between the angle measured with the analogue compass and the repeated measurements with the digital compasses is in twelve of the eighteen cases less than 10°. However, in two cases it exceeded 20°, achieving a maximum of almost 30° (29.6°) at $UC_{Central}$ with mobile device MD_1. These large errors were obtained again with small values of the standard deviation, which shows that the repeated measurements gave similar results, even though far from the correct ones.

Table 11 shows the mean of α_{Diff} ($\overline{\alpha_{Diff}}$), by mobile device MD_k ($k = 1,...,5$) considering all locations, the standard deviation of these same values ($SD(\alpha_{Diff})$), and the minimum and maximum of the absolute values of α_{Diff}, respectively, $min(\lvert \alpha_{Diff} \rvert)$ and $max(\lvert \alpha_{Diff} \rvert)$. Two mobile devices stand out as providing better results in all parameters (MD_4 and MD_5) and MD_1

showed the worse results in all parameters, very far from the mobile device with the best results MD_5. This shows how the quality of the results may vary with the mobile devices.

Table 10. α_{Analog} is the angle measured at each location with Experiment 1. $\bar{\alpha}$ is the mean value obtained for a with the n measurements, and $SD(\alpha)$ the standard deviation. α_{Diff} is the difference between α_{Analog} and $\bar{\alpha}$ (see equation (6)).

Point	Mobile device	α_{Analog}	$\bar{\alpha}$	$SD(\alpha)$	α_{Diff}
$UC_{Central}$	MD_1	90	60.4	1.2	29.6
	MD_2		92.2	1.5	-2.2
	MD_3		71.7	1.6	18.3
	MD_4		92.3	0.8	-2.3
	MD_5		92.2	0.9	-2.2
$A1_{Central}$	MD_1	90	95.1	0.7	-5.1
	MD_2		84.3	7.9	5.7
	MD_3		82.2	0.6	7.8
	MD_4		79.8	2.3	10.2
	MD_5		95.3	1.2	-5.3
$A2_{Central}$	MD_1	90	86.0	0.9	4.0
	MD_2		110.7	1.2	-20.7
	MD_3		77.7	1.3	12.3
	MD_4		83.5	0.7	6.5
	MD_5		83.8	0.9	6.2
$A3_{Central}$	MD_1	90	82.5	0.8	7.5
	MD_2		107.3	2.5	-17.3
	MD_3		87.1	1.0	2.9

Table 11. $\overline{\alpha_{Diff}}$ is the mean of α_{Diff}, computed for all location by mobile device MD_k ($k = 1,...,5$), $SD(\alpha_{Diff})$ is the standard deviation of the same values, and $min(|\alpha_{Diff}|)$ and $max(|\alpha_{Diff}|)$ are, respectively, the minimum and the maximum of the absolute values of α_{Diff}.

Mobile device	$\overline{\alpha_{Diff}}$	$SD(\alpha_{Diff})$	$min(|\alpha_{Diff}|))$	$max(|\alpha_{Diff}|)$
MD_1	11.6	12.1	4.0	29.6
MD_2	11.5	8.9	2.2	20.7
MD_3	10.3	6.6	2.9	18.3
MD_4	6.3	4.0	0.0	10.2
MD_5	4.6	2.1	0.0	6.2

4. Discussion

In this chapter we discuss the results presented in the previous chapter and point some potential solutions.

4.1. Geolocation

The errors associated with the geolocation of the mobile device will have a linear impact on the geolocation of any event whose location is determined relative to the mobile device location (see Figure 9). That is, if the event's geolocation is computed using the intersection of two contributions where the geolocation of each mobile device is measured, as well as the orientation for the event, then, the event's geolocation error due only to the mobile devices geolocation errors will generate, instead of a point, represented in Figure 9 by a flame, a circle, corresponding to the intersection of the circles representing the translation of the mobile devices geolocation errors to the event location. The resulting region is dashed in Figure 9. Therefore, errors of a few tens or even hundreds of meters won't be problematic for an application aiming to collect data about the geolocation of fires, as these are dynamic events which may have a large geographical extent and can be easily spotted when in the vicinity.
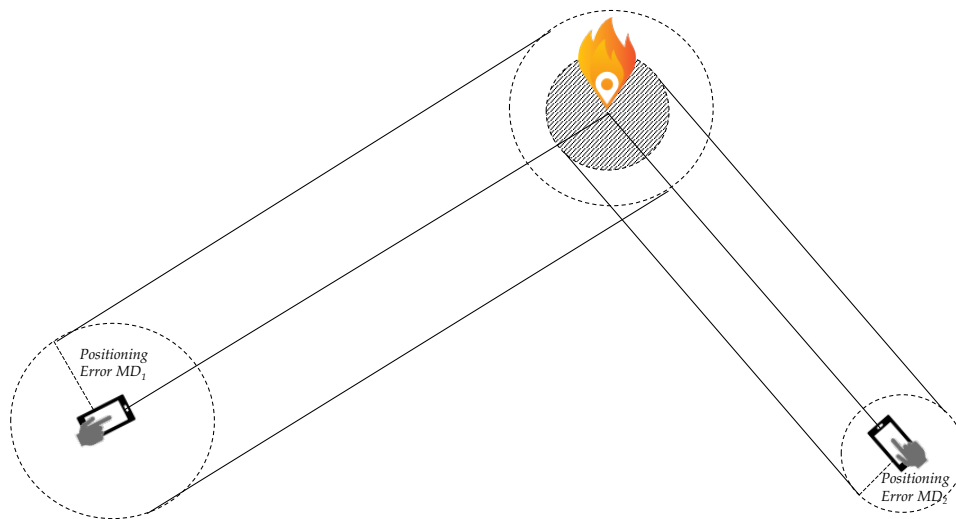
Figure 9. Influence of the mobile device's MD_1 and MD_2 positioning errors over the geolocation of the observed event (represented by a flame) if the event's location is computed with the intersection of two lines of sight and no errors in the orientation are considered.

4.2. Orientation

Regarding the implications of the orientation error, these will have a much larger impact on the geolocation of the observed events, as the impact of the measurement error increases with the distance. Figure 10 illustrates the effect of an error d in the orientation as a function of the distance.

Equation (8) may be used to estimate the magnitude of the displacement error L_i, perpendicularly to the line of sight, as a function of the distance D_i to the observed event and the orientation error d, which may be to the left or right of the orientation of interest.

$$L_i = 2D_i \sin \delta \qquad (8)$$
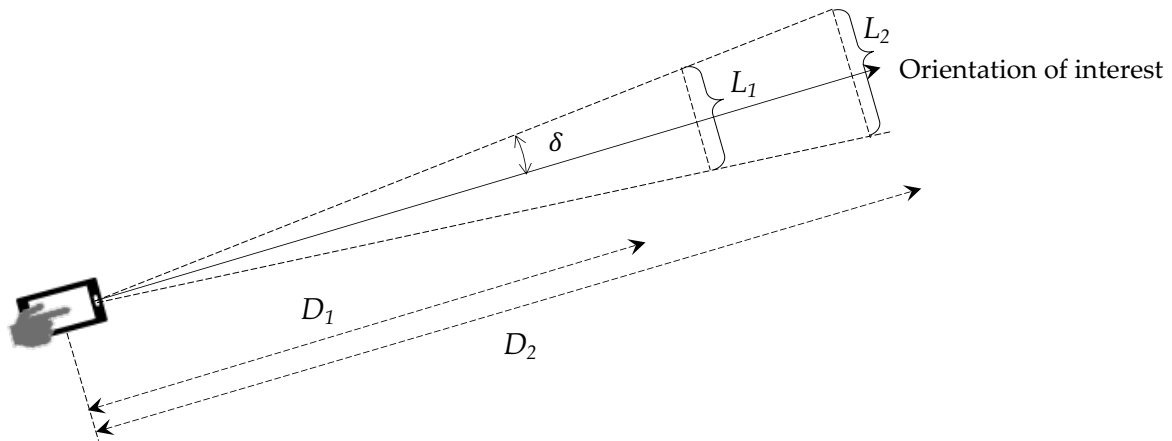
Figure 10. Orientation inaccuracy d and its potential impact L_i on fire event localization depending on its distance D_i from the observation site.

Table 12 shows the magnitude of L_i for several values of both d and D_i. The results obtained with the tests described in this paper show that in most cases the differences in the measured orientation when compared to the analogue measurements were less than 10°, which for a distance D_i of 5km corresponds to a distance L_i of 1.7 km and for a distance D_i of 10km to a distance L_i of around 3.5km, which are large but may still be useful for this type of application, as it may enable the geolocation of a fire at an early stage and in real time with an accuracy of a few kilometres. However, when the orientation error d is of a few tens of degrees and the event is some kilometres away from the observer location, L_i may reach more than 10km. The results also showed that orientation errors of these orders of magnitude may occur, and it is also possible that citizens send contributions reporting events (such as fires) that are several

kilometres away from their location. This shows that, even though this information may still be useful, orientation errors may have a considerable impact on the geolocation of the observed event, and therefore methodologies to minimize their impact need to be developed.

Table 12. Impact over the location of the observed event, expressed by distance L_i, as a function of the orientation error δ and of the distance D_i.

Angle d	Distance D_i (m)				
(degrees)	250	500	1000	5000	10000
1	9	17	35	175	349
2	17	35	70	349	698
5	44	87	174	872	1743
10	87	174	347	1736	3473
15	129	259	518	2588	5176
20	171	342	684	3420	6840
25	211	423	845	4226	8452
30	250	500	1000	5000	10000
35	287	574	1147	5736	11472
40	321	643	1286	6428	12856

4.3. Resilient Estimation

A possibility to decrease the impact of the errors identified in this paper consists in gathering various data points corresponding to a single location/orientation measurements and then perform their fusion using algorithms borrowed from the area of resilient multi-agent algorithms that aim at removing erroneous data. If a movement can be asked from the user, the approximate dynamics of the human can be used in an algorithm close to the ones presented in [31,32]. The main idea being to consider subsets of the data points and discard those whose inclusion does not conform with the asked movement. If, on the other hand, no movement can be asked, a different technique can be employed where points are ranked based on their distance to the remaining data set and low-scoring measurements are discarded as was proposed in [33].

5. Conclusions

The work presented in this paper shows the variability of the geolocation and magnetic bearing measurements when measured with five different mobile devices at four different locations. The results show that the quality of the geolocation data collected may be very different depending on the mobile devices, but the main problem appears to be the occasional

occurrence of outliers, which can be larger than 1km. When these are identified and removed from the measurements the accuracy (assessed with the mean) is in most cases less than 20m. Regarding the bearing measurements, the standard deviation of the repeated measurements is usually small (less than 1° or 2° - Tables 7, 9 and 10). However, differences relative to the true bearing may reach more than 20°, which shows that systematic errors may be present, possibly due to problems of calibration of the digital compass. These results show that to geolocate events based on the geolocation and bearing provided by mobile devices may enable the identification of a relatively large region where the event is located. Therefore, methodologies for data collection and processing should be used to minimize the influence of the measurement errors, which may include: 1) perform repeated measurements of the observer geolocation instead of collecting only one measurement of the position; 2) whenever possible perform also repeated measurements of the magnetic bearing, but more important than that is to collect the orientation for a landmark or towards a known direction, so that systematic errors in the measured orientation may be identified.

Future work includes the testing of several protocols for data collection so that the amount of data collected is maximized minimizing the steps the volunteers need to perform to collect these data, so that they are not demotivated to use the apps. This balance is important to the success of any project supported by crowdsourced data, as the availability/interest of citizens to contribute with data needs to be balanced with the effort the volunteer is available to spend to provide the data.

References

1. Kam, M.; Zhu, X.; Kalata, P. Sensor Fusion for Mobile Robot Navigation. *Proceedings of the IEEE* **1997**, *85*, 108–119, doi:10.1109/JPROC.1997.554212.

2. Yuan, Y.; Raubal, M. Exploring Georeferenced Mobile Phone Datasets – A Survey and Reference Framework. *Geography Compass* **2016**, *10*, 239–252, doi:https://doi.org/10.1111/gec3.12269.

3. Ribeiro, R.; Silvestre, D.; Silvestre, C. A Rendezvous Algorithm for Multi-Agent Systems in Disconnected Network Topologies. In Proceedings of the 2020 28th Mediterranean Conference on Control and Automation (MED); September 2020; pp. 592–597.

4. Ribeiro, R.; Silvestre, D.; Silvestre, C. Decentralized Control for Multi-Agent Missions

Based on Flocking Rules. In Proceedings of the CONTROLO 2020; Gonçalves, J.A., Braz-César, M., Coelho, J.P., Eds.; Springer International Publishing: Cham, 2021; pp. 445–454.

5. Zhang, X.; Yang, Z.; Wu, C.; Sun, W.; Liu, Y.; Xing, K. Robust Trajectory Estimation for Crowdsourcing-Based Mobile Applications. *IEEE Transactions on Parallel and Distributed Systems* **2014**, *25*, 1876–1885, doi:10.1109/TPDS.2013.250.

6. Zhang, X.; Tao, X.; Zhu, F.; Shi, X.; Wang, F. Quality Assessment of GNSS Observations from an Android N Smartphone and Positioning Performance Analysis Using Time-Differenced Filtering Approach. *GPS Solut* **2018**, *22*, 70, doi:10.1007/s10291-018-0736-8.

7. Hölzl, M.; Neumeier, R.; Ostermayer, G. Analysis of Compass Sensor Accuracy on Several Mobile Devices in an Industrial Environment. In Proceedings of the Computer Aided Systems Theory - EUROCAST 2013; Moreno-Díaz, R., Pichler, F., Quesada-Arencibia, A., Eds.; Springer: Berlin, Heidelberg, 2013; pp. 381–389.

8. Hoseinitabatabaei, S.A.; Gluhak, A.; Tafazolli, R. Towards a Position and Orientation Independent Approach for Pervasive Observation of User Direction with Mobile Phones. *Pervasive and Mobile Computing* **2015**, *17*, 23–42, doi:10.1016/j.pmcj.2014.02.002.

9. Paziewski, J. Recent Advances and Perspectives for Positioning and Applications with Smartphone GNSS Observations. *Meas. Sci. Technol.* **2020**, *31*, 091001, doi:10.1088/1361-6501/ab8a7d.

10. Dabove, P.; Di Pietra, V.; Piras, M. GNSS Positioning Using Mobile Devices with the Android Operating System. *ISPRS International Journal of Geo-Information* **2020**, *9*, 220, doi:10.3390/ijgi9040220.

11. Guo, L.; Wang, F.; Sang, J.; Lin, X.; Gong, X.; Zhang, W. Characteristics Analysis of Raw Multi-GNSS Measurement from Xiaomi Mi 8 and Positioning Performance Improvement with L5/E5 Frequency in an Urban Environment. *Remote Sensing* **2020**, *12*, 744, doi:10.3390/rs12040744.

12. Liu, Q.; Gao, C.; Peng, Z.; Zhang, R.; Shang, R. Smartphone Positioning and Accuracy Analysis Based on Real-Time Regional Ionospheric Correction Model. *Sensors* **2021**, *21*, 3879, doi:10.3390/s21113879.

13. Uradziński, M.; Bakuła, M. Assessment of Static Positioning Accuracy Using Low-Cost Smartphone GPS Devices for Geodetic Survey Points' Determination and Monitoring. *Applied Sciences* **2020**, *10*, 5308, doi:10.3390/app10155308.

14. Dabove, P.; Di Pietra, V. Towards High Accuracy GNSS Real-Time Positioning with

Smartphones. *Advances in Space Research* **2019**, *63*, 94–102, doi:10.1016/j.asr.2018.08.025.

15. Specht, M.; Specht, C.; Lasota, H.; Cywiński, P. Assessment of the Steering Precision of a Hydrographic Unmanned Surface Vessel (USV) along Sounding Profiles Using a Low-Cost Multi-Global Navigation Satellite System (GNSS) Receiver Supported Autopilot. *Sensors* **2019**, *19*, 3939, doi:10.3390/s19183939.

16. Merry, K.; Bettinger, P. Smartphone GPS Accuracy Study in an Urban Environment. *PLOS ONE* **2019**, *14*, e0219890, doi:10.1371/journal.pone.0219890.

17. Blum, J.R.; Greencorn, D.G.; Cooperstock, J.R. Smartphone Sensor Reliability for Augmented Reality Applications. In Proceedings of the Mobile and Ubiquitous Systems: Computing, Networking, and Services; Zheng, K., Li, M., Jiang, H., Eds.; Springer: Berlin, Heidelberg, 2013; pp. 127–138.

18. Olivieri de Souza, B.J.; Endler, M. Coordinating Movement within Swarms of UAVs through Mobile Networks. In Proceedings of the 2015 IEEE International Conference on Pervasive Computing and Communication Workshops (PerCom Workshops); March 2015; pp. 154–159.

19. Allmendinger, R.W.; Siron, C.R.; Scott, C.P. Structural Data Collection with Mobile Devices: Accuracy, Redundancy, and Best Practices. *Journal of Structural Geology* **2017**, *102*, 98–112, doi:10.1016/j.jsg.2017.07.011.

20. Kuhlmann, T.; Garaizar, P.; Reips, U.-D. Smartphone Sensor Accuracy Varies from Device to Device in Mobile Research: The Case of Spatial Orientation. *Behav Res* **2021**, *53*, 22–33, doi:10.3758/s13428-020-01404-5.

21. Whitmeyer, S.J.; Pyle, E.J.; Pavlis, T.L.; Swanger, W.; Roberts, L. Modern Approaches to Field Data Collection and Mapping: Digital Methods, Crowdsourcing, and the Future of Statistical Analyses. *Journal of Structural Geology* **2019**, *125*, 29–40, doi:10.1016/j.jsg.2018.06.023.

22. Novakova, L.; Pavlis, T.L. Assessment of the Precision of Smart Phones and Tablets for Measurement of Planar Orientations: A Case Study. *Journal of Structural Geology* **2017**, *97*, 93–103, doi:10.1016/j.jsg.2017.02.015.

23. Odenwald, S. *Experimeter's Guide To Smartphone Sensors*; National Aeronautics and Space Administration (NASA) Space Science Education Consortium, 2019;

24. Park, C.; Kim, I.; Jee, G.-I.; Lee, J.G. An Error Analysis of GPS Compass. In Proceedings

of the Proceedings of the 36th SICE Annual Conference. International Session Papers; July 1997; pp. 1037–1042.

25. Tomaštík, J., Jr.; Tomaštík, J., Sr.; Saloň, Š.; Piroh, R. Horizontal Accuracy and Applicability of Smartphone GNSS Positioning in Forests. *Forestry: An International Journal of Forest Research* **2017**, *90*, 187–198, doi:10.1093/forestry/cpw031.

26. Masiero, A.; Fissore, F.; Pirotti, F.; Guarnieri, A.; Vettore, A. Toward the Use of Smartphones for Mobile Mapping. *Geo-spatial Information Science* **2016**, *19*, 210–221, doi:10.1080/10095020.2016.1234684.

27. Fritz, S.; Fonte, C.C.; See, L. The Role of Citizen Science in Earth Observation. *Remote Sensing* **2017**, *9*, 357, doi:10.3390/rs9040357.

28. Foody, G.; Fritz, S.; See, L.; Mooney, P.; Olteanu-Raimond, A.-M.; Fonte, C.C.; Antoniou, V. *Mapping and the Citizen Sensor*; Ubiquity Press, 2017; ISBN 978-1-911529-18-7.

29. Compass - Apps on Google Play Available online: https://play.google.com/store/apps/details?id=app.melon.icompass&hl=en&gl=US (accessed on 17 May 2021).

30. Dados Abertos | DGT Available online: https://www.dgterritorio.gov.pt/dados-abertos (accessed on 17 May 2021).

31. Ramos, G.; Silvestre, D.; Silvestre, C. A General Discrete-Time Method to Achieve Resilience in Consensus Algorithms. In Proceedings of the 2020 59th IEEE Conference on Decision and Control (CDC); December 2020; pp. 2702–2707.

32. Ramos, G.; Silvestre, D.; Silvestre, C. General Resilient Consensus Algorithms. *International Journal of Control* **2020**, *0*, 1–15, doi:10.1080/00207179.2020.1861331.

33. Silvestre, D. Reputation-Based Method to Deal with Bad Sensor Data. *IEEE Control Systems Letters* **2020**, 1–1, doi:10.1109/LCSYS.2020.3048098.